THE INTERNATIONAL RESEARCH INSTITUTE FOR CLIMATE PREDICTION
LINKING SCIENCE TO SOCIETY

IRI TECHNICAL REPORT NO. 02-02

Improving the detection and tracking of Tropical Cyclones in Atmospheric General Circulation Models

February 2002

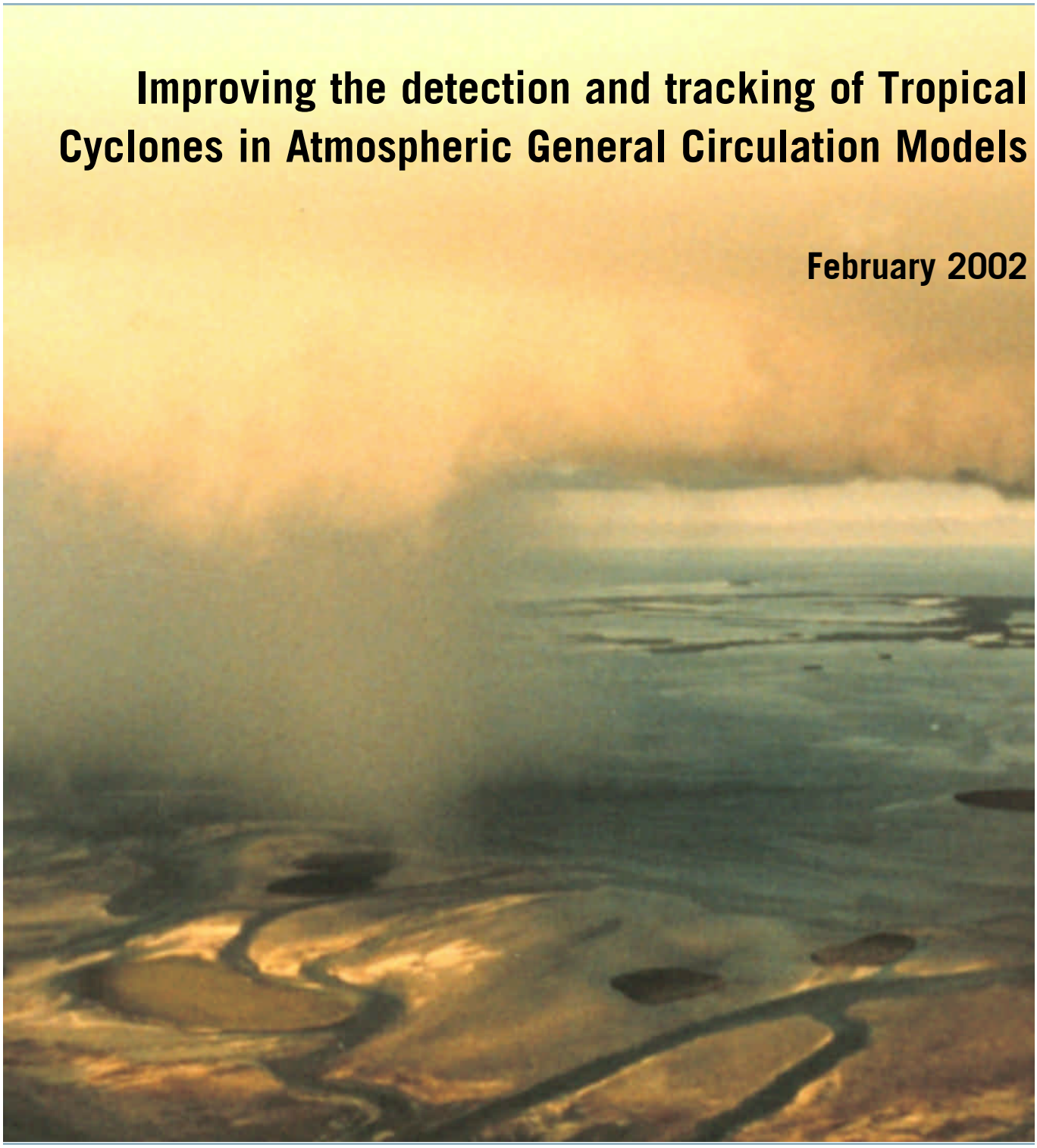

NOAA Photo Library
Lt. Debora Bari, NOAA Corps

COLUMBIA EARTH INSTITUTE
COLUMBIA UNIVERSITY IN THE CITY OF NEW YORK

Improving the detection and tracking of Tropical Cyclones in Atmospheric General Circulation Models

SUZANA J. CAMARGO AND STEPHEN E. ZEBIAK,
International Research Institute for Climate Prediction,
Lamont-Doherty Earth Observatory of Columbia University,
Palisades, NY 10964-8000

Abstract

Dynamical seasonal forecasts of tropical storm frequency require robust and efficient algorithms for detection and tracking of tropical storms in Atmospheric General Circulation Models (AGCMs). Tropical storms are generally detected when dynamic and thermodynamic variables meet specified criteria. Here, objectively defined model and basin-dependent detection criteria improve simulations of tropical storm climatology and interannual variability in low-resolution AGCMs. An improved tracking method provides more realistic tracking and accurate counting of storms.

1. Introduction

The impact of hurricanes, typhoons and tropical cyclones on society gives considerable importance to the problem of forecasting seasonal tropical cyclone frequency. Routine seasonal forecasts of tropical storm frequency in the Atlantic sector are produced using statistical methods by Colorado State University (Gray et al., 1993, 1994; Landsea et al., 1994), the Climate Prediction Center of the National Oceanic and Atmospheric Administration (CPC, 2002) and the University College of London (UCL, 2002). Statistical seasonal forecasts are also issued for the Australian sector and the Western North Pacific (Nicholls, 1992; Chan et al., 1998). Dynamical forecasting of seasonal hurricane activity using climate models is another promising approach (Bengtsson, 2001).

Seasonal AGCM prediction of large-scale variables known to affect tropical storm activity is one dynamical method of forecasting tropical storms frequency (Ryan et al., 1992; Watterson et al., 1995; Thorncroft and Pytharoulis, 2001). Another method, and the one that is the subject of this work, is based on the observation of tropical storm and cyclone-like structures in low-resolution AGCMs and coupled atmospheric-ocean models (Manabe et al., 1970; Bengtsson et al., 1982; Krishnamurti, 1988; Krishnamurti et al., 1989; Broccoli and Manabe, 1990; Wu and Lau, 1992; Haarsma et al., 1993; Bengtsson et al., 1995; Tsutsui and Kasahara, 1996; Vitart et al., 1997; Vitart and Stockdale, 2001).

Some aspects of these model tropical storms, such as their spatial and temporal distribution, are similar to observed tropical storms. The intensity of the model tropical storms is weaker and the spatial scale larger than observed due to low model resolution (Bengtsson et al., 1982; Vitart et al., 1997).

A fundamental issue is then the extent to which tropical storms in AGCM simulations represent observed climatology and interannual variability. A key element in the investigation of this issue is the objective detection and tracking of model tropical in AGCMs. Various tropical storm detection and tracking methods are reviewed in Vitart (1998). These methods are based on monitoring when chosen dynamical and thermodynamical variables exceed thresholds determined from observed

tropical storm climatologies. In previous studies (Bengtsson et al., 1982; Vitart et al., 1997), a single choice of threshold criteria was used globally, although storm statistics vary greatly from one ocean basin to another. Also, criteria taken from observational climatological values do not account for model biases. Here, we demonstrate that using basin and model dependent threshold criteria improves the climatology and interannual statistics of model tropical cyclones, thereby increasing the utility of the models.

Tracks of tropical storms in AGCMs are usually made by connecting nearby locations that satisfy the model storm detection criteria. Model tropical storms are then defined as those tracks that are longer than some fixed time interval, in most cases 1.5 - 2.0 days (Bengtsson et al., 1995; Vitart et al., 1997). Tracks defined in this manner are shorter than observed storm tracks. Such unrealistic tropical storm tracks make landfall studies difficult. Here we introduce a new tracking algorithm which extends tracks of detected storms forward and backward in time using relaxed threshold criteria. A similar idea of relaxing the thresholds for the tracking has been used in a Regional Circulation Model for the South Pacific (Nguyen and Walsh, 2001). This method allows the identification of the formation and decay of model tropical storms, information useful for studying cyclogenesis (Camargo and Sobel, 2002). Other algorithms for tracking synoptic objects in AGCMs have been previously developed for extratropical cyclones where cyclone activity is associated with strong variations in the pressure field (Williamson, 1981; Treut and Kalnay, 1990; Murray and Simmonds, 1991; Hodges, 1994; Zolina and Gulev, 2002).

The new detection and tracking algorithms have been tested with a several different AGCMs and found to improve the climatology and interannual variability compared to previous approaches (Camargo et al., 2001). The algorithms were also applied to the ECMWF Reanalysis dataset (Gibson et al., 1997; Serrano, 1997) with similar results. The tracking algorithm was also used for specific tropical cyclones in the Indian Ocean generated by a regional model (RegCM2 (Giorgi et al., 1993)) with different boundary domains (Landman et al., 2002).

We begin our discussion in Section 2 with the presentation of basin and model dependent criteria for storm detection and their application to the T42 ECHAM4.5 model (Roeckner et al.,

1996). Section 3 presents the new tracking method. Conclusions are given in Section 4. Details of the algorithms are found in the Appendices.

2. Basin-dependent detection thresholds

In the tropical storm detection methods of Vitart et al. (1997) and Bengtsson et al. (1995), tropical storms are identified by first requiring that the 850 hPa relative vorticity, the 10m wind-speed , the temperature at 850 hPa, 700 hPa, 500 hPa and 300 hPa and the sea level pressure simultaneously satisfy a set of criteria depending on several thresholds. Then nearby points are connected and classified as a tropical storm when they span at least two days. Criteria details are given Appendix A. A basin-independent version of this algorithm using the threshold values from Vitart et al. (1997) and Bengtsson et al. (1995) was applied to an ensemble of 12 integrations of the ECHAM4.5 AGCM at T42 resolution forced with observed monthly mean sea surface temperatures for the period 1979–1995. This resolution corresponds to the one used at IRI for routine seasonal forecasts (Mason et al., 1999; Goddard et al., 2001). The seven ocean basins considered follow previous studies and are shown in Fig. 1. In basins such as the Atlantic, the detection algorithm using basin-independent thresholds does not detect tropical storms found by subjective visual inspection. Also, differences in model behavior mean that thresholds appropriate for one model are not useful for another model.

We require robust methods of estimating basin and model-dependent thresholds. Here we do so by looking at the the statistical properties of the dynamic and thermodynamic variables used in the detection criteria. Since we require that the criteria be satisfied simultaneously it is useful to look at joint probability distribution functions (PDFs). Much of the relevant information can be seen in joint PDFs of vorticity/anomalous integrated temperature and vorticity/surface wind-speed. The detailed procedure used to calculate the PDFs is described in Appendix B.

In Fig. 2 the joint PDF for the low-level vorticity and the anomalous integrated temperature is shown for the Western North Pacific and Atlantic basins based on the ECHAM4.5 results. The low-level vorticity and anomalous integrated temperature are normalized in each joint PDF by the

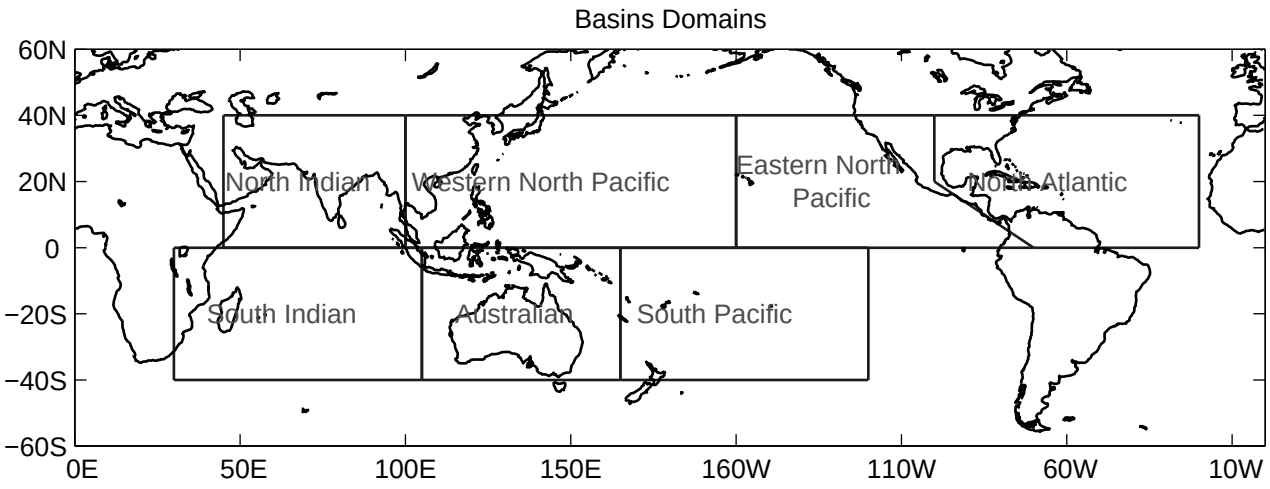

Figure 1: Definition of the ocean basins domains used in this study.

corresponding standard deviation in that ocean basin. The core portion of the two distributions is quite different. Tropical cyclones correspond to extreme values of all three of our classifying variables, and therefore occupy a small region on the periphery of the PDF domain. In the joint PDF vorticity-temperature, the tropical cyclones occur for large values of vorticity and positive integrated temperature anomalies. At higher values of vorticity, the joint PDF distribution is such that larger values of the temperature anomalies are expected. In a similar way, the joint PDF vorticity-windspeed (not shown) has a tail toward high vorticity and speed values. Tropical cyclones have all these characteristics: high vorticity, speed and positive temperature anomalies, so potentially they can be well represented by appropriate tails of theses PDFs. The PDFs are normalized by the total number of storms, so they represent a relative frequency of storms in each basin. The tails of the two distributions in normalized variables in Fig. 2 are sufficiently similar that it seems reasonable to use a single criteria in terms of the normalized variables.

Figure 2 shows that the ECHAM4.5 model has very different characteristics in the two basins shown. In the Western North Pacific (Fig. 2a) the distribution has a larger spread, with higher peak values of the vorticity, such that with a common threshold more storms would be detected. We applied the same analysis two other AGCMs (ECHAM3 (Model User Support Group, 1992) and NSIPP (Suarez and Takacs, 1995)) and to the ECMWF Reanalysis (Gibson et al., 1997) (not

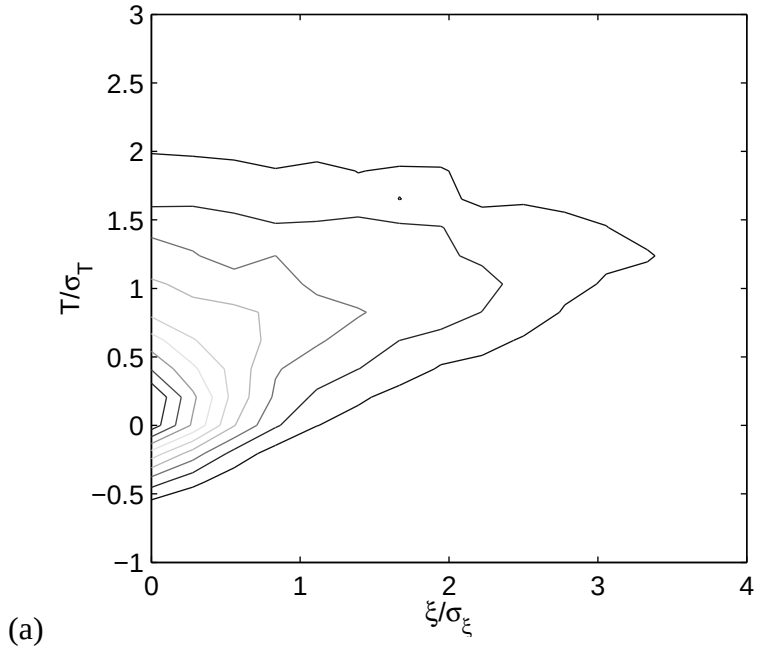

(a)

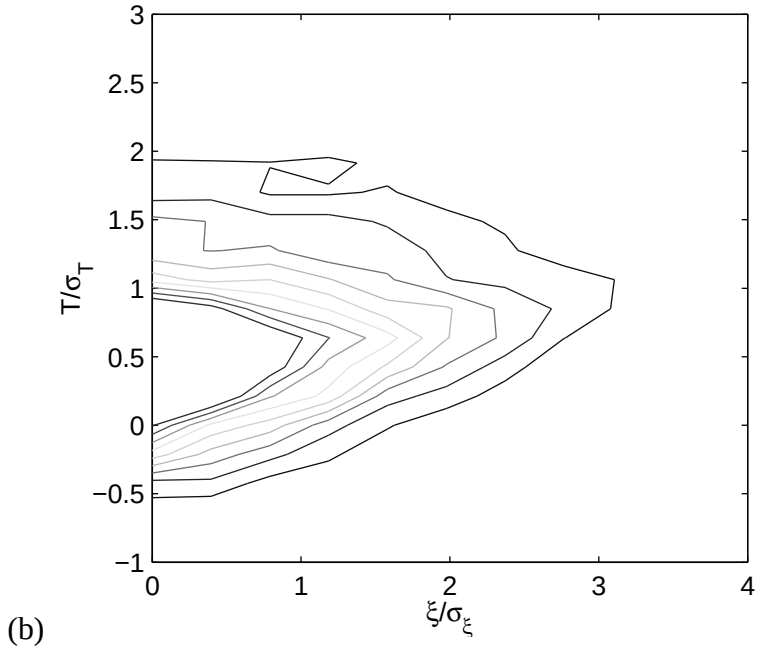

(b)

Figure 2: Joint probability distribution function (PDF) of the vorticity ξ and integrated temperature anomaly T for (a) the Western North Pacific and (b) the North Atlantic basins of the ECHAM4.5 model. In (a) and (b) the contour interval is 2×10^{-4} and 9 contour intervals were used. The variables are normalized by their respective standard deviation σ. σ_ξ values are respectively 1.3, 1.5 and σ_T are 1.9 and 2.0 in the Atlantic and Australian basin.

shown), and all the PDFs obtained have similar qualitative features in the models and in the Re-analysis. However, the numerical characteristics of the PDFs such as mean, standard deviation, maximum location are basin and model dependent. This suggests defining the detection criteria in relative terms rather than absolute terms.

Our detection algorithm is described in Appendix A. There are three variables with threshold dependent criteria: low-level vorticity, surface windspeed and integrated vertical temperature anomaly. The basin dependent threshold should reflect the different statistical characteristics of each variable and be model dependent. We chose one single parameter to define the threshold of the three variables: the standard deviation σ. However, among the variables we used as thresholds different multiples of the standard deviation, so that the basin dependent threshold would not differ greatly from the absolute thresholds. This choice allows us to have our thresholds defined from a single variable σ in a form that is consistent with observed and previous studies results, but taking into account the differing basin and model statistics.

The threshold for the vorticity in each basin ξ_{min} is the defined as $\xi_{min} = 2\sigma_\xi$, i.e. two times the standard deviation of the vorticity σ_ξ in each basin. In the case of the vertical integrated anomalous temperature, the standard deviation σ_T in each basin was calculated only among the cases that there is a warm core, in analogy to the PDFs in Appendix B. The basin dependent threshold for the vertically integrated anomalous temperature T_{min} is chosen as equal to the basin standard deviation, $T_{min} = \sigma_T$. Finally, the surface windspeed basin dependent threshold v_{min} was defined using both the windspeed standard deviation in each basin σ_v and the windspeed global average v_{gl} (calculated over ocean basins only) as $v_{min} = v_{gl} + \sigma_v$. Values of the thresholds obtained this way are shown in Table 1 together with the values used in our initial study. We note, for instance, that the thresholds are lower in the Atlantic. These parameter choices were made based on the joint PDFs statistical properties. The basin dependent threshold values so chosen are not very different from the absolute ones initially used, which were based on observational values, but at the same time reflect the different properties of the ocean basins in the models.

In Fig. 3 the effect of changing the thresholds from basin-independent to basin-dependent

	BInd	SI	AUS	SP	NI	WNP	ENP	ATL
$\xi \times 10^{-5}$	3.5	3.0	3.0	3.0	3.0	3.6	2.6	2.6
v	15	11.4	11.8	11.2	12	11.8	10.4	10.4
T	3	2.1	2.0	2.1	1.7	1.9	1.9	1.9

Table 1: Basin-independent (BInd) and basin-dependent ECHAM4.5 thresholds for vorticity, surface windspeed and integrated temperature anomaly for each of the ocean basins.

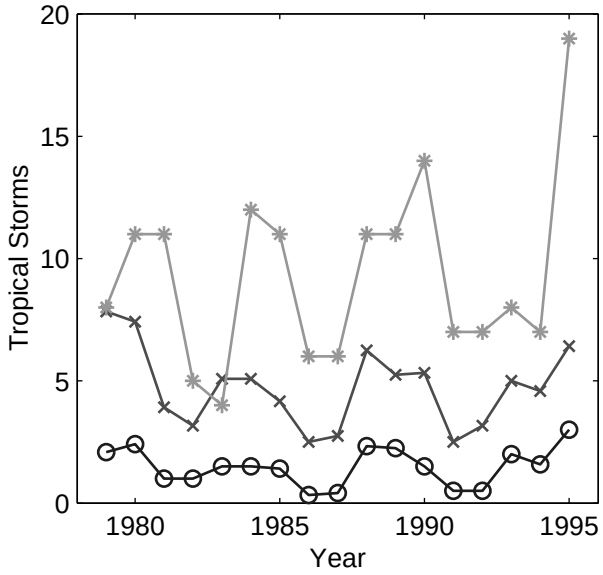

(a)

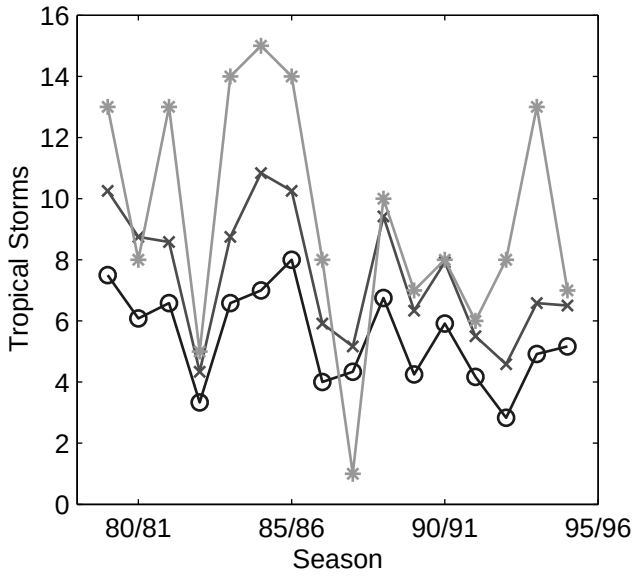

(b)

Figure 3: Ensemble mean number of storms per year detected using basin-independent thresholds (○), the basin-dependent thresholds (x) and observations (*) for the (a) Atlantic and (b) Australian basins.

Type	SI	AUS	SP	NI	WNP	ENP	ATL
Absolute	6.0	5.4	4.1	12.7	30.1	1.0	1.5
Basin dependent	9.7	7.2	5.3	11.4	36.3	4.0	3.7
Basin & Tracking	7.8	6.0	4.6	7.5	29.4	3.3	3.1
Observed	12.5	9.2	6.1	4.9	27.7	17.5	9.3

Table 2: Ensemble Average (12 members) number of storms in 17 years (1979-1995) using the old and new thresholds and the new thresholds with the new tracking algorithm.

thresholds is shown for the ensemble mean number of storms in the Atlantic and the Australian basins. In both cases, the ensemble mean number of storms increases in all years. The four regions in which the basin dependent algorithm improves the detection significantly considering all years and ensemble members are: the Atlantic (88%), Eastern Pacific (96%), South Indian (79%) and Australian (63%). The percentages were calculated using the total number of storms per year in all years and ensemble members. In these basins, the average number of storms becomes closer to observed, although the model bias is not completely corrected. The improvement of the frequency of storms occurred in all the AGCMs analysed, as the basin-dependent thresholds are also model dependent. Therefore, the detection algorithm managed to obtain better results from AGCMs taking into account the biases of each model.

With the exception of the Western North Pacific, the basin dependent thresholds produce better results than the absolute thresholds. It is important to note that we were especially concerned with the basins such as the Atlantic and Eastern North Pacific where few or no storms were being detected, and in these cases, there is a good improvement, but the model still does not produce frequencies near the observed ones.

The counting of the tropical storms can be further improved. The present algorithm counts twice a storm that weakens and strengthens again later. This problem especially affects the storm counting in the Western North Pacific due to the large number of typhoons per year. The tracking algorithm described in the next section is able to count correctly storms that weaken and strengthen again.

3. Tracking

The procedure described in Appendix A detects storms that satisfy all our criteria and connects them from one model output time to the next when they are sufficiently close, forming a storm track. However, the tracks obtained by this procedure are usually very short. Visual examination of the corresponding vorticity fields shows that the storm structure is visible well before and after the detection criteria are met. This suggests that relaxing detection criteria would produce longer tracks. However, if the detection criteria are simply relaxed uniformly, then spurious detections will also occur.

We take the first position and time where the storm meets the detection criteria and then use the low-level vorticity field to track the storm backward and forwards in time. First, the vorticity in a 5×5 grid point box is examined around the first position defined previously (based on the minimum sea level pressure), this called a vorticity matrix. The maximum value of the vorticity is found in that matrix, if in the Northern Hemisphere, a minimum for the Southern Hemisphere, and a new vorticity matrix is formed, now 3×3 grid points around this maximum. The centroid of this new vorticity matrix is then calculated and defined as the initial storm center for that storm.

Using this initial storm center the storm is then tracked backward and forward in time as follows:

- The grid point nearest the centroid center is obtained.
- A vorticity matrix 3×3 is formed in the next time step around the grid point nearest the centroid center from the previous time step.
- The absolute maximum value of the vorticity is found in this vorticity matrix and a new vorticity matrix (3×3) is defined around it.
- The position and value of the vorticity centroid of the next time step is calculated in this new vorticity matrix.

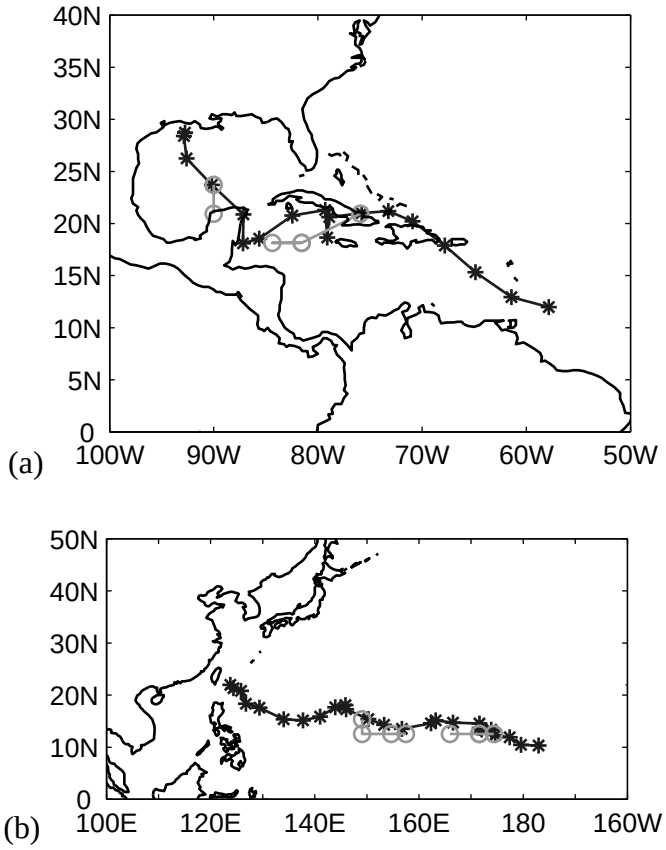

Figure 4: Tracks of a storm in the (a) Atlantic and (b) Western North Pacific using the new tracking ($*$) routine and the previous one ($\circ$).

- If the absolute value of the vorticity at the centroid at the next time step is larger than the threshold 1.5×10^{-5} this procedure is repeated.

This procedure is performed for all the storms obtained using the detection algorithm. Then, the tracks obtained are compared and if they are the same, the two storms are now counted as a single one. This procedure improves the tracks of the storms, which now are longer and more similar to observed ones. The comparison of the original tracks and the new tracks of one storm in the Atlantic and one in the Pacific is shown in Fig. 4. By examining the historical observed tracks of tropical cyclones (Unysis, 2002) and comparing to the model tracks, one finds tropical cyclones with similar paths to model tracks, while other model tracks are very different from observed ones. The new tracks are a definite improvement toward typical observed tracks.

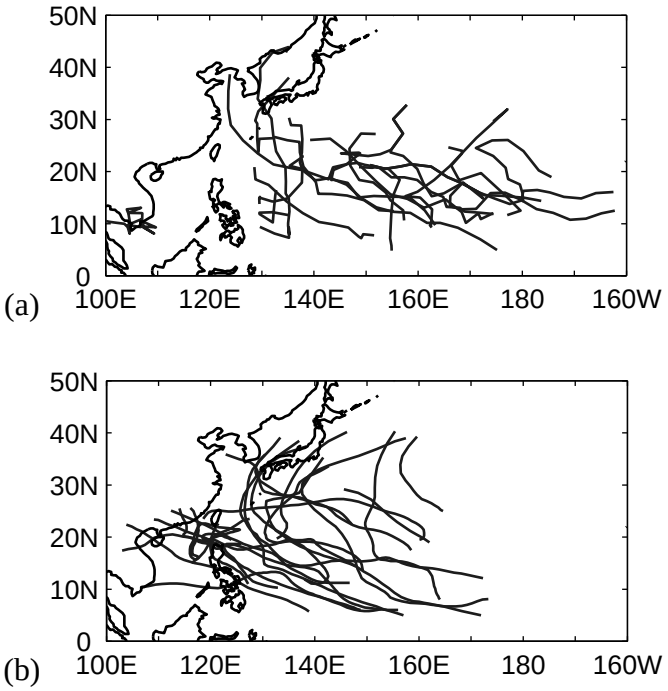

Figure 5: Tracks of all tropical storms in the Western North Pacific during the June-October 1991 typhoon season for (a) one of the ensemble members using the new tracking routine (b) observed tropical cyclones.

Figure 5a shows all the tropical storms in the Western North Pacific in one season (JJASO - June to October) for one of the ensemble members. By comparing these tracks with observed tracks in the typhoon season of the same year, shown in Fig. 5b, one sees that though the tracking algorithm improves the original tracks, the model bias is not corrected. In the Western North Pacific the model tends to form too many storms on the Central Pacific and too few in the South China Sea, compared to observed tracks. Additionally, in the Northwest basins of the Atlantic and in the Pacific, model tracks do not reach poleward latitudes as observed and most model tracks do not have the typical observed characteristic of curving around the continent as they move poleward. These model tracks biases would need to be corrected for application to landfall studies.

The counting of the storms is improved also since storms that were counted as two or three are now correctly counted as a single storm. This can be seen in Fig. 4 and Table 2, especially in the Western North Pacific. The procedure additionally makes the counting of the number of the storms

more reliable. The climatology of the storms in the different basins is improved using both the new thresholds and the new tracking procedure, as can be seen in Fig. 6, which shows the annual cycle for the model ensemble members in the South Pacific and in the Atlantic, using the previous methodology and the one described here.

4. Conclusion

Algorithms for detection and tracking of tropical cyclones in AGCMs have presented and applied to an ensemble of AGCM simulations. These algorithms use basin dependent statistics to define detection criteria thresholds and a centroid vorticity calculation to track the cyclone in time. The usage of these algorithms improves both the climatology and the tracks of tropical cyclones and therefore improves the possible use of AGCMs in forecasting seasonal cyclone frequency. Significant biases still remain and need to be addressed through increased resolution and changes in model physics. Although, this work has presented results from a single model, the algorithms have been applied successfully to several AGCMs.

Seasonal forecasts of tropical storm frequencies based on the application of these detection and tracking algorithms applied to two-tier AGCM forecasts are presently being evaluated and will be reported on in future work.

Acknowledgement The authors would like to thank Max-Planck Institute for Meteorology (Hamburg, Germany) for making their model ECHAM accessible to IRI. We thank Dr. Michael K. Tippett (IRI) for his comments on this paper.

APPENDIX A
Detection Algorithm

1. The 850 hPa relative vorticity exceeds the vorticity threshold. In the southern hemisphere a negative threshold is used.

2. The maximum surface windspeed in a centered 7×7 box exceeds the windspeed threshold.

3. The sea level pressure is the minimum in a centered 7×7 box.

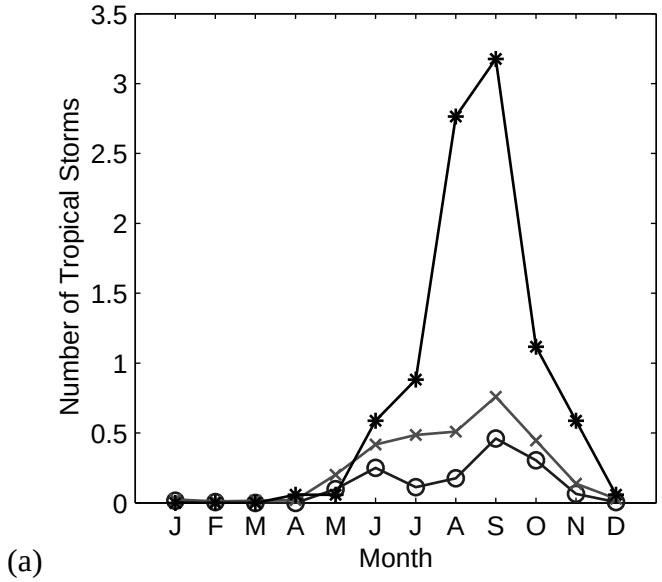

(a)

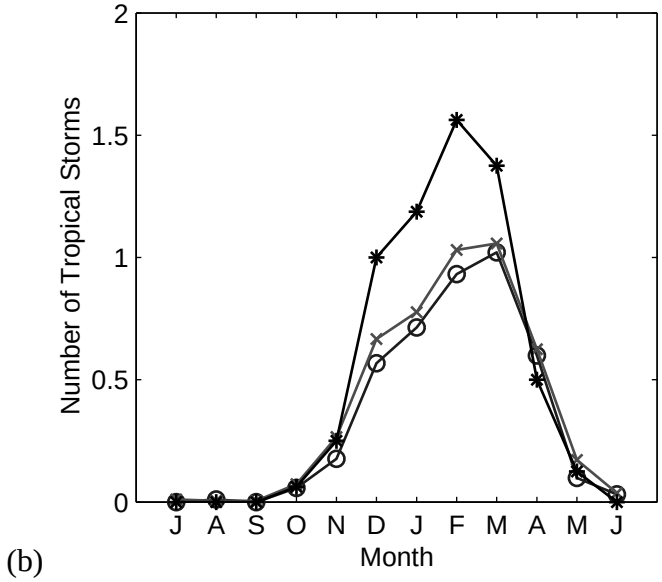

(b)

Figure 6: Annual Cycle of Tropical Storms in the (a) Atlantic (b) South Pacific using the new detection and tracking routines ($\times$) and the previous ones ($\circ$). The observed annual cycle ($\star$) is also shown.

4. The temperature anomaly averaged over the 7×7 box and the three levels: 300 hPa, 500 hPa and 700 hPa exceeds the threshold.

5. The local temperature anomaly at 300 hPa, 500 hPa and 700 hPa is positive.

6. The local temperature anomaly at 300 hPa is smaller than at 850 hPa.

7. The mean speed averaged over a 7×7 grid box is larger at 850 hPa than at 300 hPa.

8. The grid points representing the center of storms that obeyed all the criteria above are connected if they are less than a certain distance from the center of the previous time-step analyzed. This distance is defined by the frequency of the output of the model. For 6 hourly outputs, we use 2 grid points (5.6 degrees) in longitude and/or latitude, while for daily output, 3 grid points is the maximum distance (8.5 degrees) possible.

9. If the storms lasts at least 2 days (1.5 in case of 6 hourly output) identified as a model tropical storm.

APPENDIX B
Construction of the PDFs

The PDFs and statistical properties of the chosen variables (vorticity, surface windspeed and anomalous integrated temperature) are calculated in each basin using only the values during the tropical cyclone season of that basin: June - October for the Western North Pacific, Eastern North Pacific and North Atlantic; December - April for South Indian Ocean, Australian basin and South Pacific Ocean; and May, June, September, October and November for the North Indian Ocean. The points satisfy criteria 3,5 and 6. The PDFs were obtained following the procedure:

- Calculate the daily integrated temperature: sum of the temperature at 700 hPa, 500 hPa and 300 hPa in each grid point.

- A local average daily integrated temperature is calculated in a square, 7×7 grid points, centered in the grid point of interest.

- The anomalous integrated daily temperature in the grid point in the center of the square is calculated as the difference between the daily integrated temperature in that grid point and the local average daily integrated temperature around it.

- The anomalous daily temperature for the levels 850 hPa, 700 hPa, 500 hPa and 300 hPa is calculated, in analogy to the anomalous integrated temperature.

- The difference of the absolute temperature anomalies at 850 hPa and 300 hPa is calculated.

- The sign of the temperature anomalies at 700 hPa, 500 hPa and 300 hPa is compared.

- In order to be defined as having a warm core, two different criteria must be satisfied: the sign of the temperature anomalies in all three levels (700 hPa, 500 hPa and 300 hPa) must be the same, and the temperature anomaly at 850 hPa must be larger If these two criteria are not satisfied, that grid point is excluded from our statistics of the probability distribution functions and from the temperature anomalies statistics.

- The average and the standard deviation of the vorticity at 850 hPa, surface winds, and integrated temperature (only at the grid points not excluded by the previous criterion) is calculated for the time period of the integration (79-95) using the 13 ensemble members in each of the ocean basins.

- The sea level pressure value is then examined in a box of 7×7 grid points around the grid point that passed all previous criteria, if this grid point is also a local minimum, this grid point is used to construct our PDFs.

- We calculated one PDF for each ocean basin using the selected grid points integrated temperature anomaly, low level vorticity and surface windspeed. This is done for each of the basins, using all the years of the integration and all the ensemble members to construct the basin dependent PDFs.

- The vorticity at 850 hPa is than examined for the grid points that satisfy the warm core criteria, and if this in the interval of vorticity values considered, the sea level pressure value is examined in a box of 7×7 grid points around it. In case this is a local minimum, the value of the integrated temperature anomaly of surface wind speed is also examined and a probability distribution function is constructed for all the basins.

References

Bengtsson, L., 2001: Hurricane threats. *Science*, **293**, 440–441.

Bengtsson, L., H. Böttger, and M. Kanamitsu, 1982: Simulation of hurricane-type vortices in a general circulation model. *Tellus*, **34**, 440–457.

Bengtsson, L., M. Botzet, and M. Esh, 1995: Hurricane-type vortices in a general circulation model. *Tellus*, **47A**, 175–196.

Broccoli, A. J. and S. Manabe, 1990: Can existing climate models be used to study anthropogenic changes in tropical cyclone climate? *Geophys. Rev. Lett.*, **17**, 1917–1920.

Camargo, S. J. and A. H. Sobel, 2002: Western North Pacific "Tropical Cyclogenesis" in an Atmospheric General Circulation Model. *25th Conference on Hurricanes and Tropical Metereology*, San Diego, CA.

Camargo, S. J., S. E. Zebiak, and L. Goddard, 2001: Tropical storms in atmospheric global circulation models. *Proceedings of the 26th Annual Climate Diagnostics and Prediction Workshop*, San Diego, CA.

Chan, J. C. L., J. E. Shi, and C. M. Lam, 1998: Seasonal forecasting of tropical cyclone activity over the Western North Pacific and the South China Sea. *Wea. Forecasting*, **13**, 997–1004.

CPC, 2002: http://www.cpc.ncep.noaa.gov.

Gibson, J. K., P. Källberg, S. Uppala, A. Hernandez, A. Nomura, and E. Serrano, 1997: ERA Description. ERA PR1, European Centre for Medium-Range Weather Forecasts.

Giorgi, F., M. R. Marinucci, and G. T. Bates, 1993: Development of a 2nd-Generation Regional Climate Model (REGCM2).1. Boundary-layer and Radiative-transfer Processes. *Mon. Wea. Rev.*, **121**, 2794–2813.

Goddard, L., S. J. Mason, S. E. Zebiak, C. F. Ropelewski, R. E. Basher, and M. A. Cane, 2001: Current approaches to seasonal to interannual climate predictions. *Int. J. Climatol.*, **21**, 1111–1152.

Gray, W. M., C. W. Landsea, P. W. M. Jr., and K. J. Berry, 1993: Predicting Atlantic Basin Seasonal Tropical Cyclone Activity by 1 August. *Wea. Forecasting*, **8**, 73–86.

—, 1994: Predicting Atlantic Basin Seasonal Tropical Cyclone Activity by 1 June. *Wea. Forecasting*, **9**, 103–115.

Haarsma, R. J., J. F. B. Mitchell, and C. A. Senior, 1993: Tropical disturbances in a GCM. *Clim. Dyn.*, **8**, 247–257.

Hodges, K. I., 1994: A General Method for Tracking Analysis and Its Application to Meterological Data. *Mon. Wea. Rev.*, **122**, 2573–2586.

Krishnamurti, T. N., 1988: Some recent results on numerical weather prediction over the tropics. *Aus. Meteor. Mag.*, **36**, 141–170.

Krishnamurti, T. N., D. Oosterhof, and N. Dignon, 1989: Hurricane prediction with a high resolution global model. *Mon. Wea. Rev*, **117**, 631–669.

Landman, W. A., A. Seth, and S. J. Camargo, 2002: The Effect of Regional Climate Model Domain Choice on the Simulation of Tropical Cyclones Statistics in the Southwestern Indian Ocean, in preparation.

Landsea, C. W., W. M. Gray, P. W. M. Jr., and K. J. Berry, 1994: Seasonal forecasting of atlantic hurricane activity. *Weather*, **49**, 273–284.

Manabe, S., J. L. Holloway, and H. M. Stone, 1970: Tropical Circulation in a Time-Integration of a Global Model of the Atmosphere. *J. Atmos. Sci.*, **27**, 580–613.

Mason, S. J., L. Goddard, N. E. Graham, E. Yulaeva, L. Q. Sun, and P. A. Arkin, 1999: The IRI seasonal climate prediction system and the 1997/98 El Nino event. *Bull. Amer. Meteor. Soc.*, **80**, 1853–1873.

Model User Support Group, 1992: Echam3 - atmospheric general circulation model. Technical Report 6, Das Deutshes Klimarechnenzentrum, Hamburg, Germany.

Murray, R. J. and I. Simmonds, 1991: A numerical scheme for tracking cyclone centres from digital data, Part I: Development and operation of the scheme. *Aust. Meteor. Mag*, **39**, 155–166.

Nguyen, K. C. and K. J. E. Walsh, 2001: Interannual, Decadal and Transient Greenhouse Simulation of Tropical Cyclone-like Vortices in a Regional Climate Model of the South Pacific. *J. Climate*, **14**, 3043–3054.

Nicholls, N., 1992: Recent performance of a method for forecasting australian seasonal tropical cyclone activity. *Aust. Meteor. Mag.*, **39**, 155–166.

Roeckner, E., K. Arpe, L. Bengtsson, M. Christoph, M. Claussen, L. Dümenil, M. Esch, M. Giorgetta, U. Schlese, and U. Schulzweida, 1996: The atmospheric general circulation model ECHAM-4: Model description and simulation of present-day climate. Technical Report 218, Max-Planck Institute for Meteorology.

Ryan, B. F., I. G. Watterson, and J. L. Evans, 1992: Tropical cyclone frequencies inferred from Gray's yearly genesis parameter: Validation of GCM tropical climate. *Geophys. Res. Lett.*, **19**, 1831–1834.

Serrano, E., 1997: Tropical cyclones. ECMWF Re-Analysis Project Report Series 5, European Centre for Medium-Range Weather Forecasts.

Suarez, M. J. and L. L. Takacs, 1995: Documentation of the Aries/GEOS dynamical core Version 2. Technical Memorandum 104606, 5, NASA, Greenbelt, MA.

Thorncroft, C. and I. Pytharoulis, 2001: A Dynamical Approach to Seasonal Prediction of Atlantic Tropical Cyclone Activity. *Wea. Forecasting*, **16**, 725–734.

Treut, H. L. and E. Kalnay, 1990: Comparison of observed and simulated cyclone frequency distribution as determined by an objective method. *Atmösfera*, **3**, 57–71.

Tsutsui, J. I. and A. Kasahara, 1996: Simulated tropical cyclones using the national center for atmospheric research community climate model. *J. Geophys. Res.*, **101**, 15013–15032.

UCL, 2002: http://forecast.mssl.ucl.ac.uk.

Unysis, 2002: http://weather.unisys.com.

Vitart, F., 1998: *Tropical storm interannual and interdecadal variability in an ensemble of GCM integrations*. Ph.D. thesis, Princenton University.

Vitart, F., J. L. Anderson, and W. F. Stern, 1997: Simulation of Interannual Variability of Tropical Storm Frequency in an Ensemble of GCM Integrations. *J. Climate*, **10**, 745–760.

Vitart, F. D. and T. N. Stockdale, 2001: Seasonal forecasting of tropical storms using coupled GCM integrations. *Mon. Wea. Rev.*, **129**, 2521–2537.

Watterson, I. G., J. L. Evans, and B. F. Ryan, 1995: Seasonal and Interannual Variability of Tropical Cyclogenesis: Diagnostics from Large-scale Fields. *J. Climate*, **8**, 3042–3066.

Williamson, D. L., 1981: Storm track representation and verification. *Tellus*, **33**, 513–530.

Wu, G. and N. C. Lau, 1992: A GCM Simulation of the Relationship Between Tropical Storm Formation and ENSO. *Mon. Wea. Rev.*, **120**, 958–977.

Zolina, O. and S. K. Gulev, 2002: Improving the Accuracy of Mapping Cyclone Numbers and Frequencies. *Mon. Wea. Rev.*, **130**, 748–759.